Underwater localization and node mobility estimation

Saif Khalid Mudhafar, Ammar Ebdelmelik Abdelkareem
Department of Computer Networks Engineering, College of Information Engineering, Al-Nahrain University, Baghdad, Iraq

Article Info

ABSTRACT

In this paper, localizing a moving node in the context of underwater wireless sensor networks (UWSNs) is considered. Most existing algorithms have had designed to work with a static node in the networks. However, in practical case, the node is dynamic due to relative motion between the transmitter and receiver. The main idea is to record the time of arrival message (ToA) stamp and estimating the drift in the sampling frequency accordingly. It should be emphasized that, the channel conditions such as multipath and delay spread, and ambient noise is considered to make the system pragmatic. A joint prediction of the node mobility and speed are estimated based on the sampling frequency offset estimation. This sampling frequency offset drift is detected based on correlating an anticipated window in the orthogonal frequency division multiplexing (OFDM) of the received packet. The range and the distance of the mobile node is predicted from estimating the speed at the received packet and reused in the position estimation algorithm. The underwater acoustic channel is considered in this paper with 8 paths and maximum delay spread of 48 ms to simulate a pragmatic case. The performance is evaluated by adopting different nodes speeds in the simulation in two scenarios of expansion and compression. The results show that the proposed algorithm has a stable profile in the presence of severe channel conditions. Also, the result shows that the maximum speed that can be adopted in this algorithm is 9 km/h and the expansion case profile is more stable than the compression scenario. In addition, a comparison with a dynamic triangular algorithm (DTN) is presented in order to evaluate the proposed system.

Corresponding Author:

Saif Khalid Mudhafar
Department of Computer Networks Engineering, College of Information Engineering, Al-Nahrain University
Baghdad, Jadiria, P.O. Box 64004, Iraq
Email: saif.khalid@coie-nahrain.edu.iq

1. INTRODUCTION

Earth is a planet of blue. About 71 percent of the Earth's surface is occupied by water, equivalent to an area of 361 million km^2 and 1:3 billion km^3 of thickness. This vastness is still unexplored and remains a mystery. The need for powerful and efficient underwater wireless networks is rising increasingly to discover the fascinating world of the undersea [1], [2].

Underwater acoustic communications (UAC) are generally considered as the most viable alternative at acceptable distances, among the different means of communication. The earliest UAC originates from the need for military uses. UAC is used for communications between submarines during World War II, and the modulation of the analog one-sideband suppressed-carrier amplitude is introduced [1]. Localization in many applications is one of the most common technologies, although it plays an essential role. Motivated by widespread localization adoption, in this paper, we provide a detailed of the localization algorithms. Next, we group localization algorithms into different groups based on range based and free based algorithms [3]–[5].

The location of underwater sensor networks, handheld sensor nodes are essential. For some applications, such as marine monitoring, highly accurate localization is required while some applications such as surveillance require localization solution [5]–[7]. An underwater wireless sensor network (UWSN) is one of the new sciences emerging in latest years and important to many researchers who are mainly interested in the wireless sensor network (WSN) area. UWSNs are a series of sensors and vehicles distributed widely or in an efficient manner, linked with the acoustic wave, under the relatively moving water surface. Associated to the acoustic wave. UWSN is a powerful aquatic mechanism used for numerous purposes, such as monitoring fish farms, coral and ocean life, prediction of disasters and military purposes [8].

Underwater data transmission between sensor nodes, for example, optical wave, electromagnetic wave and acoustic wave which can be achieved in crosswise over optical and electromagnetic wave. Data transmission using underwater light not propagated for long distance and the acoustic waves are the most suitable way of transmitting data over long distance underwater as well as consuming fewer energy than optical and electromagnetic wave, however, the characteristics of acoustic sensor propagation underwater and mobility pose great challenges to high precision and scalable localization solutions [8]–[13]. In this paper, we analyzed the working mechanisms and techniques provided by localization and speed prediction in underwater wireless sensor.

2.   LITERATURE REVIEW

Underwater wireless sensor network has been a research field for quite some time to come. A lot of research is going on in this area as it has wide applications ranging from oceanography to early warning systems for natural disasters (such as tsunamis), monitoring of wildlife, oil exploration, and military surveillance. In recent years, many researchers have studied the localization and prediction of mobility node.

A survey of major curricula and methods are presented briefly. Here are a few of the works which were read and reviewed. Erol *et al.* [14] suggested dive "N" rise schemes for localization. The scheme assumes that to evaluate their z-coordinate, the dive "N" rise (DNR) beacons and ordinary nodes are fitted with pressure sensors. DNR's key concept is for each beacon system to rise the surface to get its location from global positioning system (GPS). Then it dives underwater while transmitting its location coordinates in a straight vertical direction. For range calculations, every ordinary node uses these packets for location. Then, to estimate its location, the bounding box or triangulation methods are used. In spite its ease, it takes longer to dive and ascend the DNR beacons; therefore, the speed and coverage of the area relies largely on the beacons' speed and their amounts. Due to the slow speed of the location process of the DNR, which is mostly caused by the slow speed of the DNR beacons, scheme of multi-stage localization (MLS) is proposed. It implements an iterative process so that the ordinary nodes that are located serve as reference nodes and can communicate their position coordinates to help locate other nodes. Using literation process, they are used localization of three packets from three sources non-collinear to approximate node position. Although MLS increases the speed of localization and the cost of rollout, this is done at the expense of high position error and high overhead communication.

Langowski [15] presented the proposition of the carrier frequency monitoring algorithm and sampling frequency offsets. The algorithm uses a phase difference between estimates of the channel transfer function, determined for two successive orthogonal frequency division multiplexing (OFDM) symbols for the same subcarrier. The suggested solution is contrasted with a popular non-data-aided algorithm implemented by computer simulation, resulting in smaller carrier frequency offset (CFO) and sampling frequency offset (SFO) mean square error (MSE) estimates than the reference algorithm.

Zhou *et al.* [16] proposed an area-based localization scheme (ALS). The ALS measures the location of the nodes within a given region rather than providing an exact position of the nodes. Its mechanism is as, buoy on surface transmits beacon packets at various levels of power and at differing time periods.

Once these beacons are received, the sensor nodes report the lowest power level of each received anchor node. Then it sends this data on to the sink nodes on the floor. This data is used by sink nodes to estimate the region of the sensor. The range and granularity of ALS is restricted by the number of anchor nodes and their positions, the number of transmitted power levels and their magnitudes. Moreover, node mobility is not approved by the system, only the assumes 2D world.

Zhou *et al.* [17] in this article, predictable mobility patterns is used for underwater objects, they suggest a scheme for underwater sensor networks, called scalable localization scheme with mobility projection (SLMP). Localization is done in such a hierarchical way in SLMP, and the entire process of localization is split into two parts: localization of anchor nodes and localization of ordinary nodes. Each node predicts its future mobility trend based on its previously established location information during the localization process, and it may estimate its future location based on its projected mobility pattern. Anchor nodes with defined positions in the network will monitor the entire process of localization to balance the tradeoff between precision of localization, scope of localization and cost of communication. They perform

extensive simulations, and they finding that SLMP can significantly mitigate the localization communication cost while retaining relatively good localization coverage and precision.

Han *et al.* [3] present a detailed survey of localization algorithms in this article. Firstly, on the basis of the sensor nodes mobility, they divide localization algorithms into three main categories: hybrid, stationary, and mobile localization algorithms. Finally, they are discussing in details the localization algorithms and evaluate potential localization algorithm research directions in UWSNs. A distributed localization framework is suggested Bhoopathy *et al.* [18], that uses a two-way method of arrival time estimation to measure distance and prevent the time synchronization constraint. This method overcomes the issue of versatility and thereby reduces the connectivity costs and the total network latency.

Beniwal *et al.* [19] proposed a localization scheme called time synchronization localization scheme (LSWTS). LSWTS constitutes an enhancement over the DNR system by eliminating the time synchronization condition. After receiving their positioning information from GPS swim, the DNR beacons vertically underwater and transmit packets of localization within a period of time. An ordinary node passively listens to these packets, and it measures its distance to the beacon as it receives two localization packets from a beacon system at two different time points. If then the node decides its distances to three beacons, the trilateration method is used to approximate its position. While LSWTS locates nodes without time synchronization, its range based on the quantity and allocation of the beacon nodes, as it allows at least 3 beacon nodes to be positioned within the coverage each node.

In study Zhang *et al.* [20], the range-based particle swarm optimization (PSO) algorithm is used in the proposed approach to find the beacon nodes, and it is possible to quantify their speeds. Using the spatial similarity of the underwater object moving, the velocity of an unknown node is measured, and then its position can be estimated. The range-based PSO algorithm can cause major consumption of energy and the difficulty of its computation has been a little bit high, this approach can obviously minimize the consumption of energy and cost of time of locating these mobile nodes. This approach has higher precision of position and a greater degree of coverage of localization.

Yan *et al.* [21] present an asynchronous localization algorithm with mobility prediction for underwater acoustic sensor networks (UASNs). The algorithm includes the mobility of sensor nodes with the help of autonomous underwater vehicles (AUVs), an asynchronous algorithm for sensor nodes to localize themselves, and an iterative least squares method to solve the optimization problem. Based on simulations and analysis of the Cramer-Rao lower bound, this algorithm can eliminate the effect of asynchronous clock, and achieve the predicted performance in localization of mobile underwater sensor nodes and reduce the localization time and eliminate the impact of the clock asynchronization and node mobility.

In order to identify the error and precision of localization of sensor, Su *et al.* [4] present a general localization algorithm and then deploy the ordinary beacon nodes. After that, they present two localization algorithms called distance-based and angle-based algorithms. The results exhibit that this algorithm compensates for time synchronization, estimate the mean errors in localization and achieve good localization accuracy.

Guo *et al.* [22] analyzed the features of nodes with mobile beacons limited and recommends a new UWSN location algorithm, Mobile-constrained localization algorithm based on beacons. It resolves the problem of dynamic and imprecise beacon node position. The unknown node may be positioned between the location of the anchor and the traveling radius of the beacon node by geometric reference. The polygonal region is converted into a rectangular area during the calculation process, and the three dimensional are translated into a two-dimensional space, the process of calculation is streamlined and the algorithm's feasibility is improved. The algorithm can be used for localization of both 2D and 3D. Results of the experiment demonstrate that the suggested algorithm in this paper increases the precision of localization, decreases the rate of error of the network nodes position and has great practicability.

Shakila and Paramasivan [23] proposed method to the range-based whale optimization algorithm (WOA). Localization error is further minimized to calculate the valued location of the sensors. By adding the WOA in this job, the localization error is minimized. Results of replication indicate that introduction metrics of the intended technique beat those of the present work as far as constraint error and inclusion of restrictions is concerned. In comparison, the new scheme achieves greater coverage of localization.

3. SYSTEM MODEL

The transmitted packet adopted in the simulation is shown in Figure 1. One of the major reasons to select the OFDM is to reduce the effect of the frequency selectivity of the underwater channel. Moreover, the periodicity feature of the cyclic prefix orthogonal frequency division multiplexing (CP-OFDM) is exploited to detect the position of the maximum peak of lag and differentiate the channel from the signal affected by the channel. The proposed structure contains an overhead composite: 20 ms linear frequency modulation

signal, 54 ms silent period followed by an OFDM frame of 356 ms for the purpose of simulation. The reason behind selecting the LFM is to mitigate the effectiveness of the inherent Doppler shift as well as the ambient noise of the environment.

In order to estimate the sampling frequency drift, the time of arrival (ToA) is adopted. It is assumed that the transmitted packet time from the node is T_{TP} which is known. At the reciver node, the packet arrived at time T_{RP}. Based on the packet arrival time, the samples drift is computed. There were some common parameters adopted to deal with acoustic signal which utilized in the proposed system as in depicted in Table 1. All these parameters simulated in MATLAB.
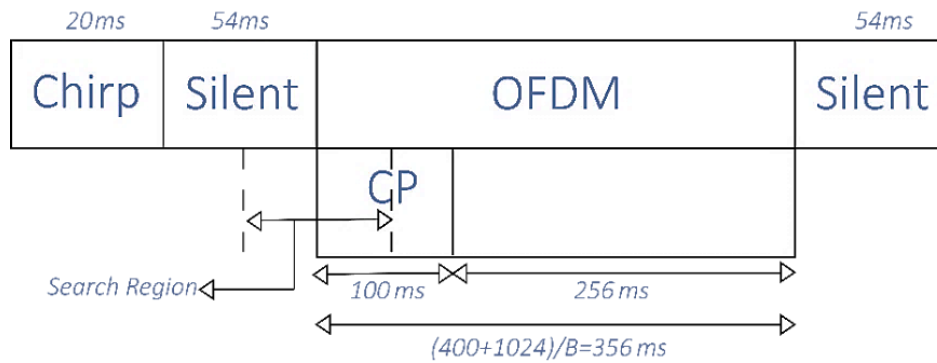

Figure 1. Packet structure

Table 1. Simulation parameters in MATLAB

Parameter	Value
Transmission Frequency Band	8-16 KHz
Bandwidth	4 KHz
Delay Spread	48 ms
Number of Sub-carriers	1024
Number of cycle prefix	400
Number of Samples/Symbol	12
Guard interval	50 ms
Silent period	54 ms
Linear frequency modulation (LFM)	20 ms
Sampling Frequency	48KHz
Signal-to-noise ratio (SNR)	5 dB

4.   SAMPLING FREQUENCY ESTIMATION

For the purpose of estimating the sampling frequency drift, it is crucial to estimate the scaling factor $(1 + \Delta)$ at the reciver. It should be emphasized that the sampling frequency change has an impact on all paths in the channel. It is well known that the node mobility manifests its self as the signal dilation and/or compression, thus the scaling factor is adopted to estimate change in the sampling interval $T_{st} = \frac{T_{sy}}{N_c}$ in sender node where T_{sy} is the OFDM symbol time and N_c is number of sub-carriers. Thus, the received drifted samples signal can be modeled as in (1) [24]:

$$y_r(t) = x_{tr}\left[(1 \pm v_c)t - \tau_{pt}\right] \tag{1}$$

where v_c is relative motion between two nodes and τ_{pt} is time varying path delay. Converting (1) to discrete time, a scaled received signal waveform can be represented as in (2) [14]:

$$y_r[kT_{TP}] = x_{tr}[k(1 \pm \Delta)T_{TP}] \tag{2}$$

where, k is an integer, T_{TP} is time interval of the received packet, $x_{tr}(kT_{TP})$ is the sampled transmitted signal, and $y_r(kT_{TP})$ is drifted samples received signal.

The negative sign indicates that one node is moving towards another node (packet compression). This case results in decreasing the distance between them. Whereas the positive sign indicates that the node is moving away and ultimately increasing the distance between them. However, it should be emphasized that in

both cases, the OFDM symbol time is shifted nonuniformly. Thus, the received (drifted samples) packet can be modeled as in (3) [24]:

$$T_{RP} = T_{TP} \pm \delta \qquad (3)$$

where T_{RP} is the received packet time, T_{TP} is a transmitted time stamp, and δ is the samples offset. For this reason, two scenarios are considered, see subsection 4.1 and 4.2.

4.1. Expansion case

This scenario is considered when the nodes are diverging. Regardless which node is moving away as shown in Figure 2, the consequence in that the number of samples in the transmitted packet will be increased, thus the packet time is consequently increased. This dilation due to the movement of current waves or the ship that are very close the nodes. Then the sampled frequency can be represented as in (4) [24]. As shown in Figure 1, the search region is to find the drift in these samples.
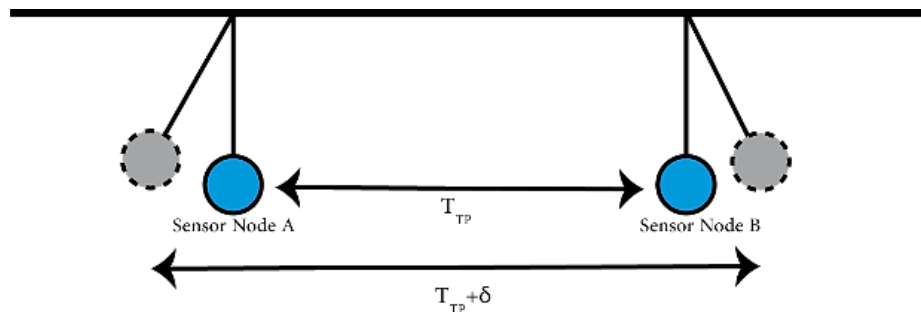
$$\hat{f}_s = f_s(1 + \frac{v_c}{c}) \qquad (4)$$

Figure 2. Expansion scenario

4.2. Compression case

On the other hand, the compression scenario is considered when the two nodes are converging. This case necessitates to find the how many samples are lost in the received packet. This case causes a severe scenario compared with the expansion case as shown in Figure 3. The delivered packet to the node at the receiver is affected by its sampling frequency as in (5) [24].

$$\hat{f}_s = f_s(1 - \frac{v_c}{c}) \qquad (5)$$

It is obvious from (5) that the estimating sampling frequency $\hat{f}_s$ is equal to the transmitted sampling frequency when ther is no movement in the nodes, i.e, v_c=0. However, this not the actual case where, the mobile node changes the transmitted sampling frequency by the factor of $\frac{v_c}{c}$, which results in an unescaleable sampling frequency. This case is shown in Figures 3 and 4, where the peaks are drifted to the left. These samples that are drifted δ to the left or right from the center is estimated using the correlation in (6). It should be emphasized that this drift requires to be compensated to receive reliable data, however, this paper is interesting to estimate these samples to detect the node position. As shown in (7) the samples drift δ is obtained by correlating the samples within a search window. This is in the help of the cyclic prefix property, where it delivers a high correlation characteristic.

Due to the periodicity of the cyclic prefix, their samples are well correlated whilst the remaining samples are remaining mutually uncorrelated. The autocorrelation after the band pass filter (BPF) in the front end receiver can be expressed as in (6) [24]:

$$r_{yy}(\delta) = \sum_{i=1}^{N_c} y_r(i)y_r(i-\delta) \qquad (6)$$

where δ=0, $\pm 1, \pm 2, \pm 3, \ldots$. The autocorrelation argument in (7) results in an approximation of the samples drift and represented as:

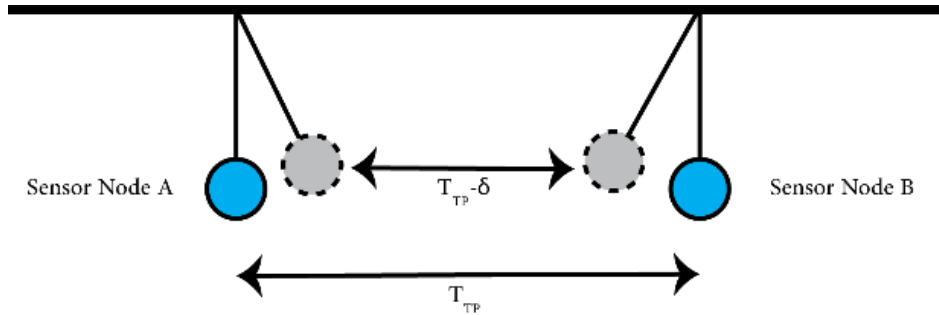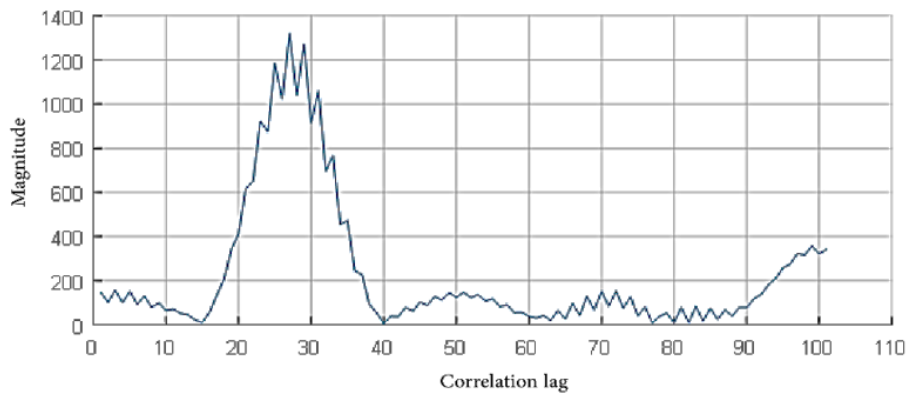$$\delta_{peak} = \arg\max r_{yy}(\delta) \tag{7}$$

Figure 3. Compression scenario

Figure 4. Autocorrelation of $|r_{yy}|$ for lag detection at 3 m/s

In Figure 4 it is noticed that there is an uncertainty in the peaks position. For this reason, the envelope of the correlation should be smoothed in order to improve the detection. This is evidence that the sampling frequency drift can be seen by the frame length in terms of dilation or compression. Accordingly, exploiting the samples' drift in estimating the speed is now feasible. To accomplish this, let κ be the sampling frequency offset due to one sample drift, which can be formulated as in (8) [24]:

$$\kappa = \frac{N_c T_{st}}{(1+\Delta)T_{sr}} \tag{8}$$

where, the sender symbol interval duration T_{st} is known and received symbol interval duration T_{sr} is estimated.

5.   JOINT NODE SPEED PREDICTION AND LOCALIZATION

For joint estimation, the sampling frequency offset in (8) is exploited for two purposes. Speed estimation which is utilized at the same time as the radius of the circle to reach the predicted node. Thus, the speed can be approximated as in (9) [24].

$$\tilde{v_c} = [1 - (1 + \Delta)] * c \tag{9}$$

From the relation between (8) and (9), it can be demonstrated that the samples drift is proportional to the estimated relative velocity as in (10) [24].

$$\tilde{v_c} = \left(1 - \frac{\kappa T_{sr}}{N_c T_{st}}\right) * c \tag{10}$$

Underwater localization and node mobility estimation (Saif Khalid Mudhafar)

According to the estimated speed in (10), we could estimate the coordinates for S sensor nodes. In this paper, it is assumed that the mobile node's location is within the mapping circle identified by the estimated speed. This is a pragmatic scenario because the speed of the mobile node is covered by the propagation speed underwater. The estimation of these coordination based on the mapping circle, where the distance d1 between mobile node and master node is carefully predicted. In this scenario, improved dynamic triangular algorithm (DTN) [25] is utilized. Unlike [25], the radius of the mapping circle is predicted using (10) which reduce the complexity of using the received signal strength (RSS). The angle from both references (mobile node and master node) to point (x3, y3) is then measured using DTN in [25]. Since the pairs (x1, y1) and (x3, y3) are known, measurement of angle gives all the information required to determine the equations of the lines joining point 3 to the reference locations. The intersection yields (x2, y2) as shown in Figure 5.
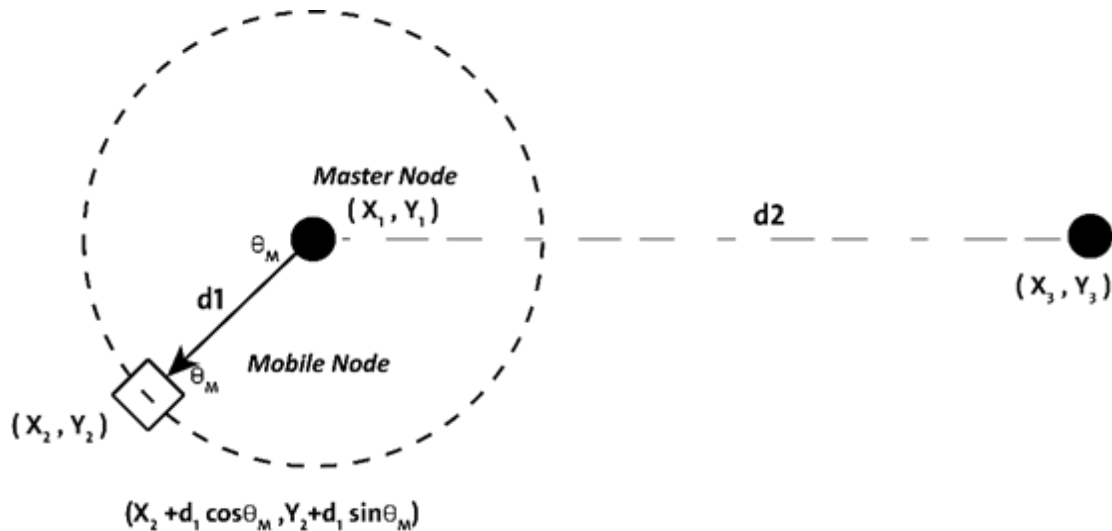

Figure 5. Determination of new point using angle measurement

6. THE PROPOSED ALGORITHM

The following steps represent the proposed algorithm of finding the estimated speed $\tilde{v_c}$: i) read receive signal, ii) filter the received signal using band-pass filter, iii) start frame detection, iv) autocorrelation within anticipated window $r_{yy}(\delta)$, v) find maximum peak and location $\delta_{peak} = \arg\max r_{yy}(\delta)$, vi) drive scaling factor $(1+\Delta)$, vii) find the estimated speed $\tilde{v_c}$, and viii) run DTN algorithms.

7. THE ALTERNATIVE DTN ALGORITHM

In the alternative method, the DTN was proposed to find the coordinates of the mobile users indoor on the terrestrial channel. In order to operate on this algorithm, it is required to conduct of at least 3 sensor nodes, and in the case of using more than the default number such as 4 nodes of sensing, the algorithm will neglect the weaker RSS received signal and the sensor that receives the largest signal is designated as a reference node. Assuming that the mobile user is within a circle, so that the distance between the reference node and the mobile user is then calculated. In the proposed technique, this distance is estimated as it is recognized manually in the alternative, the angle is calculated and then the coordinates of the mobile user are founded. Gray prediction (GP) system was also used to estimate the value of the inclination of the signal, and this system also reduces the fluctuations of the signal, which was also applied in this work. Also the spread of the radio signal in the building is easily affected by the reflection, diffraction and dispersion of obstacles generated by the radio [25].

In the proposed system, the DTN algorithm and GP system were effectively applied in an underwater environment to find the coordinates of the mobility sensor node. As for the distance between the mobile node and the reference node, we made an automatic join by using the estimated speed m/s through our program instead of the value of (r), which represents the radius of the mobility node. Moreover, In the proposed system in an underwater environment, we use an acoustic sensor node instead of an radio frequency (RF).

Additionally, we added multipath channel and additive white Gaussian noise (AWGN) noise. It is noticed that the proposed algorithm has a stable profile. This is because the estimated speed accuracy helps in the estimation of the coordinates. This is realistic as the node is moving in a speed compatible with the coordination.

7.1. The alternative DTN algorithm steps

The following steps represent the dynamic triangular algorithm of finding the location of mobility node: i) read estimated speed and assume it as the radius of circle that mobility node search through it, ii) generate received signal strength indicator (RSSI) using estimated speed, iii) finding strongest RSSI, and iv) generating mapping circle using (11) [25]:

$$X_{th}, Y_{th} = X_{p1} + d_1 \cos\theta, Y_{p1} + d_1 \sin\theta \tag{11}$$

where it represents the estimation coordinate of X, Y.
- Pick up the strong RSSI to estimate the distance between master node and mobility node using (12) [23].

$$d_1 = d_0 \, 10^{\frac{RSSI_0 - RSSI_M}{10^n}} \tag{12}$$

- Finding the coordinates of mobility node using (13) [25].

$$D(X, Y) = X_{p1} + d_1 \cos\theta, Y_{p1} + d_1 \sin\theta \tag{13}$$

- Calculating the residual error $f_{(u,i)}$ between the range measurement and the distance to the initially estimated position using (14) [25].

$$f_{i,u} = r_{i,u-} \sqrt{(x_i - x_u^\wedge)^2 + (y_i - y_u^\wedge)^2} \tag{14}$$

where X_{th}, Y_{th}: the mapping circle to find the possible location; $d_\circ$: the initial distance; d_1: the estimated distance; X_{p1}: the predicted X axis; Y_{p1}: the predicted Y axis; and $D(X, Y)$: the estimation coordinates.

8.   RESULTS AND ANALYSIS

In the simulation, the transmitted packet shown in Figure 1 and the system specifications were used. In this paper, the OFDM symbol was designed to suit the underwater channel characteristics. Thus, for a delay spread of 50 ms, the transmitted packet was protected with a long cyclic prefix. A packet length of 17,088 samples were transmitted where the packet length is calculated from (15):

$$\left(N_c + N_{cp}\right) \times N_s \tag{15}$$

where N_c is number of sub-carriers, N_{cp} is number of cycle prefix, and N_s is number of samples/symbols.

It should be emphasized that considering this packet structure for the purpose of tackling the drift in the sampling frequency, however, sacrificing the data rate. In order to evaluate the proposed technique, two scenarios were considered: expansion and compression. In both cases, the two nodes (master node and the mobile node) that diverged from another or converged between the sensor's nodes, respectively. Low speed [±9 km/h] and node coordinates estimations that associate the node mobility are considered in the proposed scenarios. The aforementioned parameters are evaluated under the following channel characteristics [24]. The channel impulse response over 8 path and maximum delay spread about 48 ms can be represented:

$$h(n) = 0.9\delta(n - 7) + 0.75\delta(n - 6) + 0.75\delta(n - 5) + 0.7\delta(n - 4) + 0.6\delta(n - 3)$$
$$+0.6\delta(n - 2) + 0.55\delta(n - 1) + 0.45\delta(n)$$

and the time delays at $n - 7$ to n be 0, 0.5, 1, 2, 30, 34, 46.5, 48.3 ms. This channel is presented in Figure 6. In this Figure, it can be seen that the maximum delay spread is up to 48 ms. However, based on closer look of the impulse response that the channel is sever as the are many paths are very close to each other whereas some paths have longer delay spread and semi-identical magnitude. It can be inferred from the frequency response shown in Figure 7 that the channel is severe and there is a selectivity in the frequency.
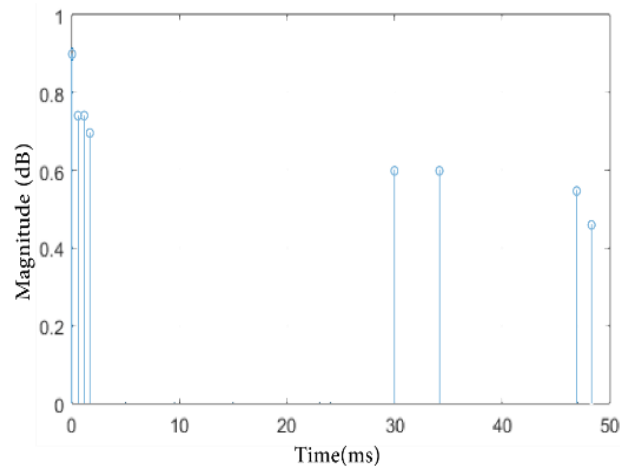
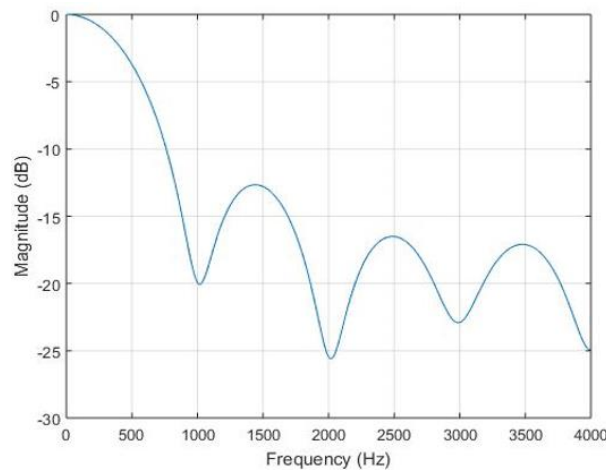Figure 6. Channel impulse response for the simulation

Figure 7. Channel frequency response

8.1. Dilation scenario

This scenario when the mobility sensor node is moving away from the master node (anchor node). That's mean the transmitted signal manifests itself as an expanded signal to the receiver (mobile node). A low-speed case is investigated in both speed and coordination estimation.

8.1.1. Speed estimation at three sensors nodes

In Table 2, it can be shown that the speed is predicted based on the time scaling factor estimation for low speeds of the sensor nodes. The performance of the proposed system is satisfied for calculating speed estimation. In Figure 8, the scaling factor is varying according to the direction of the movement. Besides that, it can be seen in Figure 9 the speed is changing linearly up to 9 km/h accordingly. Furthermore, it is evident that delivering the estimated speed to the coordination algorithm is capable of tracking the change in node position due to the mobility. However, uncertainty in estimating the coordination in the negative speed is due the effect of the channel on the correlation peak.

Table 2. The performance of dilation case at sensor=3, (X,Y)=3,3

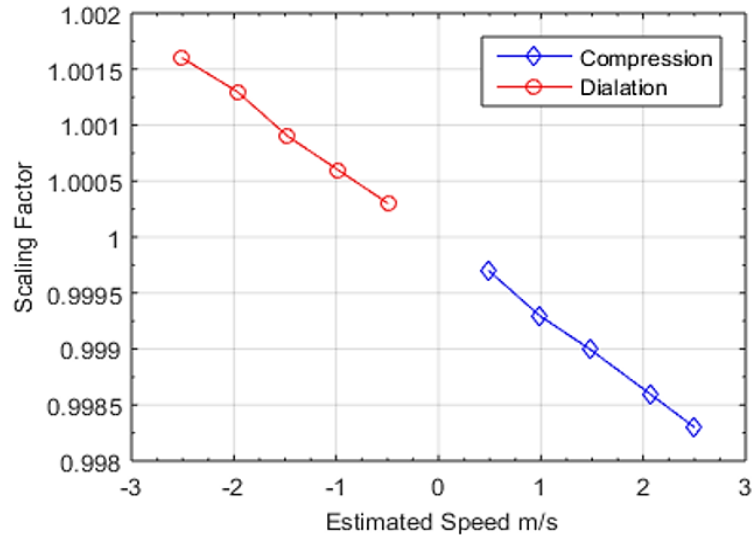| Speed (m/s)	Estimated speed (m/s)	X Coordinates	Y Coordinates	$f_{(u,i)}$	Scaling factor
0.5	0.4902	3.2592	3.2549	0.127	0.9997
1.0	0.9804	3.4834	3.5142	0.275	0.9993
1.5	1.4735	3.8006	3.7327	0.388	0.9990
2.0	2.0633	4.0293	4.0800	0.571	0.9986
2.5	2.5000	4.2466	4.2864	0.709	0.9983

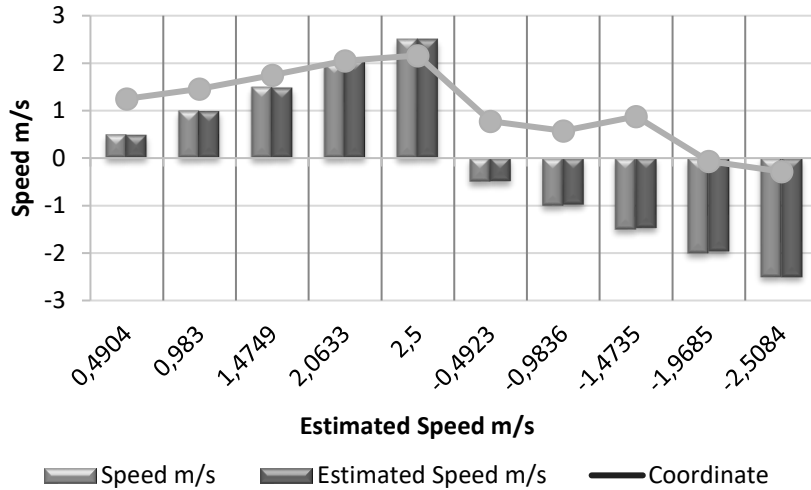Figure 8. Estimated scaling factor and associated speed

Figure 9. Estimated speed with associated coordinates at sensor=3

8.1.2. Coordination estimation

In Table 1, the coordination of the predicted node is also estimated based on the estimated speed. In our scenario, the reference node i is (X,Y)=3,3 and the number of sensors S=3. This reference is used to computing the position given estimated speed information within the mapping circle. It is considered that the estimated speed represents the range of the node with unknown position u. An error between the range measurement (estimated speed) and distance (between the reference node and the predicted coordinates) is also measured. As shown in the table, the residual error $f_{(u,i)}$ is calculated using (14). It can be noticed that the error is increased proportional to the speed.

8.1.3. Speed and coordination estimation when using four sensors node

In Table 3, the performance of the proposed system is perfectly work when using 4 sensors as it will province more flexibility to select the strongest signal. In this scenario, the number of sensors S=4 was used and the reference node i is (X, Y) =3,3, and the DTN algorithm will neglect the weakest signal RSSI, and this algorithm will assign the sensor node that receives the largest signal to be designated as the main reference node. It can be seen in Figure 10; the coordination of the predicted node is also estimated based on the estimated speed. This reference is used to computing the position given estimated speed information within the mapping circle.

Table 3. The performance of dilation case at sensor=4, (X, Y)=3,3

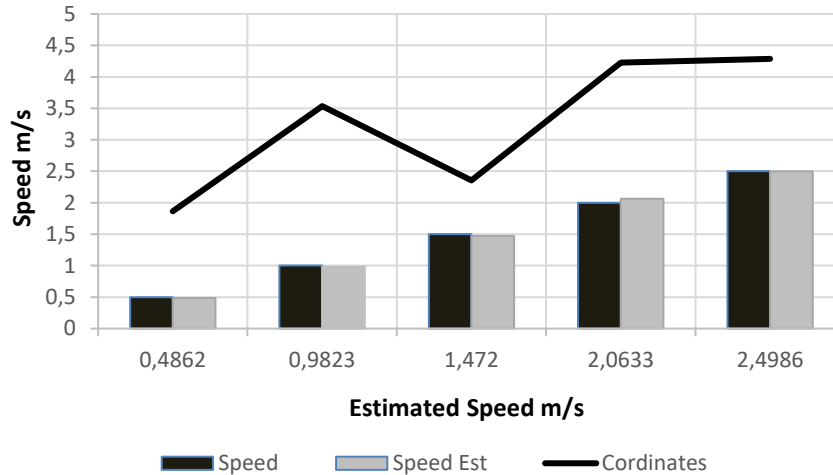| Speed (m/s)	Estimated speed (m/s)	X Coordinates	Y Coordinates	$f_{(u,i)}$	Scaling factor
0.5	0.4862	2.4288	1.8639	-0.7854	0.9997
1.0	0.9823	3.5516	3.5332	0.21512	0.9993
1.5	1.4720	3.0277	2.3559	0.827305	0.9990
2.0	2.0633	4.2089	4.2252	0.342093	0.9983
2.5	2.4986	4.2482	4.2863	0.706235	0.9983

Figure 10. Estimated speed with associated coordinates at sensor=4

8.2. Compression scenario

This scenario when the sensor node is moving toward the master node. In this case, the nodes are converged and the transmitted signal is compressed. According to the node velocity (-ve) speed, the samples length is reduced. Thus, a change in the time scaling factor is occurred, which increased proportionally with the speed.

8.2.1. Speed estimation

In Table 4, the speed is of (-) sign. This is due to that the scaling factor is increased. It can be seen from the table that at compression case, the proposed system performance achieves a stable profile in terms of speed estimation.

Table 4. The performance of compression case at sensor=3, (X,Y)=1,1

Speed (m/s)	Estimated speed (m/s)	X Coordinates	Y Coordinates	$f_{(u,i)}$	Scaling factor
-0.5	-0.4926	2.7691	2.7375	-0.842	1.0003
-1.0	-0.9836	-3.4351	2.4739	-7.440	1.0006
-1.5	-1.4735	-5.1128	5.7266	-10.032	1.0009
-2.0	-1.9659	-3.8658	1.8892	-8.921	1.0013
-2.5	-2.5084	-5.0942	3.4531	-10.615	1.0016

8.2.2. Coordination estimation

The error in (14) is also computed. Unlike the expansion scenario, the error is high in the compression scenario. This is due to the speed estimation problem in the case of moving node towards the reference, which caused a fractional sample. The reason behind this comes from the cyclic prefix correlation, where reducing the symbol time length and increasing the channel effect. Furthermore, reducing the symbol length set a burden on the search region and the correlation to detect the maximum peak and causes false alarm. Consequently, the coordination estimation is weak in the compression case.

In order to evaluate the proposed system performance, a comparison in Figure 11 is presented. In this Figure, it is noticed that the proposed algorithm has more stable profile in underwater than terrestrial WSN. This is because the estimated speed accuracy helps in the estimation of the coordinates. This is realistic as the node is moving in a speed compatible with the coordination.
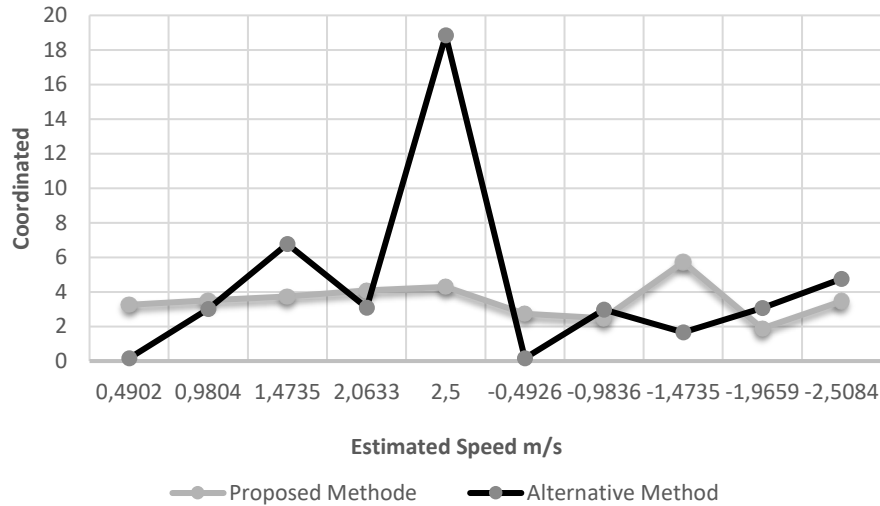
Figure 11. Performance comparison between the proposed and alternative at sensor=3

9.   THE PROPOSED METHOD LIMITATION

The comparison of node speeds estimation is shown in Figure 12, the reference node *i* is (X, Y) =1,1 and the number of sensors S=3. It demonstrates that the proposed technique is failed to estimate the high node speeds accurately, as present in Table 5 and 6 for the dilation and compression scenario respectively. The coordination of the predicted node is also estimated based on the estimated speed leads to inaccuracies in locating the node. This is realistic because the node is moving at a high speed which cannot be calculated in the proposed system. Note that Table 6 shows that the window we are searching through for the estimated speed in the compression scenario, the search will be narrow as the (*-ve*) speed increases, and the channel effect will be more and thus will affect the detection.
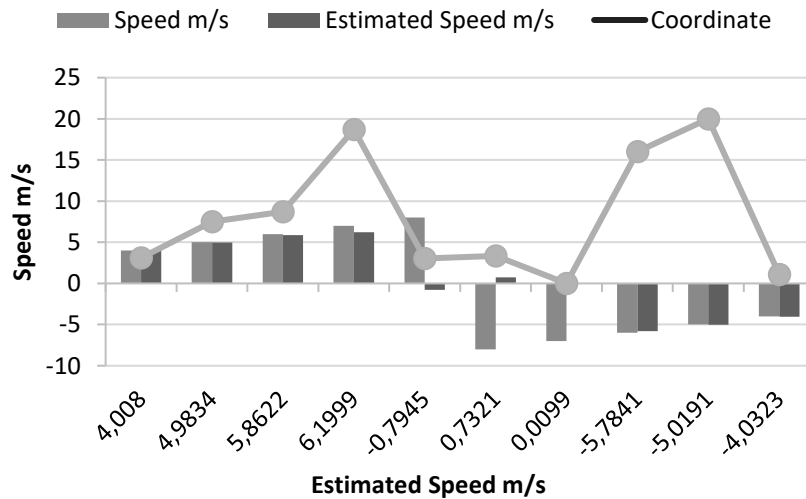

Figure 12. Estimated speed with associated coordinates at sensor=3 for high speed

Table 5. The performance of dilation at sensor=3, (X1,Y1)=1

Speed (m/s)	Estimated speed (m/s)	X Coordinates	Y Coordinates	Scaling factor
4	4.008	4.9670	3.0924	0.9973
5	4.9834	21.172	7.5002	0.9967
6	5.8622	28.693	8.7021	0.9961
7	6.1999	30.000	18.683	0.9958
8	-0.7945	3.0120	3.0120	1.0004

Table 6. The Performance of compression at sensor=3, (X1,Y1)=1

Speed (m/s)	Estimated speed (m/s)	X Coordinates	Y Coordinates	Scaling factor
-4	-4.0323	0.9391	1.0951	1.0026
-5	-5.0191	-17.5391	20.000	1.0033
-6	-5.7841	-20.2685	16.000	1.0037
-7	0.0099	0.02320	0.0040	1.0000
-8	0.7321	3.40040	3.3330	0.9995

10. DISCCUSION OF RESULTS

The estimated speed of mobility node is calculated using sampling frequency offset by driving scaling factor. The location of mobility node is calculated using DTN algorithms where the distance between the anchor node and mobility node is calculated. The results show that the proposed algorithm jointly estimates the speed and location and has more stability than DTN with severe channel conditions.

11. CONCLUSION

Node coordination and speed are jointly estimated and presented in this paper. Two scenarios Dilation and compression were adopted and evaluated. Results show that the proposed algorithm succeeded in estimating a low-speed movement of the node mobility up to ±9 km/h. This speed is reused in estimating the position of the mobile node. Comparison shows that the proposed technique is investigated through simulation and it outperforms the alternative method and has a stable profile. In order to mimic the real case, both scenarios are assessed with 8 paths channel and maximum delay spread of 48 ms. It has been concluded that the estimation in the case of expansion outperforms the estimation of the position in the compression. One of the most important challenges to be considered is estimating the position of the mobile node in higher speed. Furthermore, the proposed algorithms failed to calculate the precision location due to inaccuracy in the estimated speed.

REFERENCES

[1] X. Cheng, L. Yang, and X. Cheng, *Cooperative OFDM underwater acoustic communications*. 2016, doi: 10.1007/978-3-319-33207-9.

[2] M. Ahmed, M. Salleh, M. I. Channa, and M. F. Rohani, "Review on localization based routing protocols for underwater wireless sensor network," *International Journal of Electrical and Computer Engineering (IJECE)*, vol. 7, no. 1, pp. 536–541, Feb. 2017, doi: 10.11591/ijece.v7i1.pp536-541.

[3] G. Han, J. Jiang, L. Shu, Y. Xu, and F. Wang, "Localization algorithms of underwater wireless sensor networks: a survey," *Sensors*, vol. 12, no. 2, pp. 2026–2061, Feb. 2012, doi: 10.3390/s120202026.

[4] X. Su, I. Ullah, X. Liu, and D. Choi, "A review of underwater localization techniques, algorithms, and challenges," *Journal of Sensors*, vol. 2020, pp. 1–24, Jan. 2020, doi: 10.1155/2020/6403161.

[5] P. V. Amoli, "An overview on researches on underwater sensor networks: Applications, current challenges and future trends," *International Journal of Electrical and Computer Engineering (IJECE)*, vol. 6, no. 3, pp. 955–962, Jun. 2016, doi: 10.11591/ijece.v6i3.9201.

[6] M. B. S. Halakarnimath and D. A. V Sutagundar, "Localization in Underwater Acoustic Sensor Networks using Trapezoid," *International Journal of Recent Technology and Engineering (IJRTE)*, vol. 8, no. 5, pp. 186–193, Jan. 2020, doi: 10.35940/ijrte.E5695.018520.

[7] P.-H. Tsai, R.-G. Tsai, and S.-S. Wang, "Hybrid localization approach for underwater sensor networks," *Journal of Sensors*, vol. 2017, pp. 1–13, 2017, doi: 10.1155/2017/5768651.

[8] E. M. Sozer, M. Stojanovic, and J. G. Proakis, "Underwater acoustic networks," *IEEE Journal of Oceanic Engineering*, vol. 25, no. 1, pp. 72–83, Jan. 2000, doi: 10.1109/48.820738.

[9] S. Wang, Y. Lin, H. Tao, P. K. Sharma, and J. Wang, "Underwater acoustic sensor networks node localization based on compressive sensing in water hydrology," *Sensors*, vol. 19, no. 20, Oct. 2019, doi: 10.3390/s19204552.

[10] M. C. Joyce and K. Vanitha, "Deployment model of an underwater sensor network in a swimming pool environment with a suitable localization scheme," *International Journal of Scientific and Engineering Research*, vol. 5, no. 9, pp. 286–291, 2014

[11] M. Zorzi, P. Casari, N. Baldo, and A. Harris, "Energy-efficient routing schemes for underwater acoustic networks," *IEEE Journal on Selected Areas in Communications*, vol. 26, no. 9, pp. 1754–1766, Dec. 2008, doi: 10.1109/JSAC.2008.081214.

[12] A. E. Abdelkareem, B. S. Sharif, and C. C. Tsimenidis, "Adaptive time varying doppler shift compensation algorithm for OFDM-based underwater acoustic communication systems," *Ad Hoc Networks*, vol. 45, pp. 104–119, Jul. 2016, doi: 10.1016/j.adhoc.2015.05.011.

[13] A. E. Abdelkareem, B. S. Sharif, C. C. Tsimenidis, and J. A. Neasham, "Time varying doppler-shift compensation for OFDM-based shallow underwater acoustic communication systems," in *IEEE Eighth International Conference on Mobile Ad-Hoc and Sensor Systems*, Oct. 2011, pp. 885–891., doi: 10.1109/MASS.2011.105.

[14] M. Erol, L. F. M. Vieira, and M. Gerla, "Localization with Dive'N'Rise (DNR) beacons for underwater acoustic sensor networks," *Proceedings of the Second Workshop on Underwater Networks (WuWNet '07)*, 2007, doi: 10.1145/1287812.1287833.

[15] A. Langowski, "Carrier and sampling frequency offset estimation and tracking in OFDM systems," *SoftCom 2008: 16th International Conference on Software, Telecommuncations and Computer Networks*, vol. 5, no. 2, pp. 319–323, 2008, doi: 10.1109/SOFTCOM.2008.4669503.

[16] Y. Zhou, B. Gu, K. Chen, J. Chen, and H. Guan, "An range-free localization scheme for large scale underwater wireless sensor

networks," *Journal of Shanghai Jiaotong University (Science)*, vol. 14, no. 5, pp. 562–568, Oct. 2009, doi: 10.1007/s12204-009-0562-9.

[17]   Z. Zhou, Z. Peng, J.-H. Cui, Z. Shi, and A. Bagtzoglou, "Scalable localization with mobility prediction for underwater sensor networks," *IEEE Transactions on Mobile Computing*, vol. 10, no. 3, pp. 335–348, Mar. 2011, doi: 10.1109/TMC.2010.158.

[18]   V. M. Bhoopathy, M. B. H. Frej, S. R. E. Amalorpavaraj, and I. Shaik, "Localization and mobility of underwater acoustic sensor nodes," in *Annual Connecticut Conference on Industrial Electronics, Technology and Automation (CT-IETA)*, Oct. 2016, pp. 1–5, doi: 10.1109/CT-IETA.2016.7868249.

[19]   M. Beniwal, R. P. Singh, and A. Sangwan, "A localization scheme for underwater sensor networks without time synchronization," *Wireless Personal Communications*, vol. 88, no. 3, pp. 537–552, 2016, doi: 10.1007/s11277-016-3175-2.

[20]   Y. Zhang, J. Liang, S. Jiang, and W. Chen, "A localization method for underwater wireless sensor networks based on mobility prediction and particle swarm optimization algorithms," *Sensors*, vol. 16, no. 2, Feb. 2016, doi: 10.3390/s16020212.

[21]   J. Yan, X. Zhang, X. Luo, Y. Wang, C. Chen, and X. Guan, "Asynchronous localization with mobility prediction for underwater acoustic sensor networks," *IEEE Transactions on Vehicular Technology*, vol. 67, no. 3, pp. 2543–2556, Mar. 2018, doi: 10.1109/TVT.2017.2764265.

[22]   Y. Guo, Q. Han, and X. Kang, "Underwater sensor networks localization based on mobility-constrained beacon," *Wireless Networks*, vol. 26, no. 4, pp. 2585–2594, May 2020, doi: 10.1007/s11276-019-02023-5.

[23]   R. Shakila and B. Paramasivan, "An improved range based localization using whale optimization algorithm in underwater wireless sensor network," *Journal of Ambient Intelligence and Humanized Computing*, vol. 12, no. 6, pp. 6479–6489, Jun. 2021, doi: 10.1007/s12652-020-02263-w.

[24]   B.-C. Kim and I.-T. Lu, "Parameter study of OFDM underwater communications system," in *OCEANS 2000 MTS/IEEE Conference and Exhibition*, 2000, vol. 2, pp. 1251–1255., doi: 10.1109/OCEANS.2000.881774.

[25]   R. C. Luo, Chen, and S. H. Pan, "Mobile user localization in wireless sensor network using grey prediction method," in *Annual Conference of IEEE Industrial Electronics Society, 2005*, 2005, vol. 2005, doi: 10.1109/IECON.2005.1569330.

BIOGRAPHIES OF AUTHORS

Saif Khalid Mudhafar received the B.Sc. in physics degree from Al-Mustansiriyah University, Iraq, in 2010 and the B.Sc. degree in Network Engineering from Al-Iraqia University, Iraq, in 2017 and the M.Sc. degrees in Networks Engineering and Internet Technologies, Underwater localization and node mobility estimation engineering from Al-Nahrain University, Iraq, Baghdad, in 2020. He can be contacted at email: saif.khalid@coie-nahrain.edu.iq.

Ammar Ebdelmelik Abdelkareem received the B.Sc. and M.Sc. degrees in computer engineering from the University of Technology, Baghdad, Iraq, in 1992 and 2002, respectively. He received the Ph.D. degree from Newcastle University, England, 2012. Currently, he is working lecturer at Al-Nahrain University, Iraq. His research interests include computer architectures, signal processing for Underwater communications, digital signal processors (DSPs), and embedded systems using SHARC processor. He can be contacted at email: ammar.algassab@nahrainuniv.edu.iq.